Human Molecular Genetics, 2017, Vol. 26, No. 18 3495–3507

doi: 10.1093/hmg/ddx235
Advance Access Publication Date: 20 June 2017
Original Article

ORIGINAL ARTICLE

Age-dependent effects of *Armc5* haploinsufficiency on adrenocortical function

A. Berthon[1], F.R. Faucz[1], S. Espiard[2], L. Drougat[1], J. Bertherat[2,3] and C.A. Stratakis[1,*]

[1]Section on Endocrinology and Genetics, *Eunice Kennedy Shriver* National Institute of Child Health and Human Development, National Institutes of Health, Bethesda, MD 20892, USA, [2]Institut Cochin, INSERM U 1016, CNRS UMR8104, Université Paris Descartes, 75014 Paris, France and [3]Department of Endocrinology, Referral Center for Rare Adrenal Diseases, Assistance Publique Hôpitaux de Paris, Hôpital Cochin, 75014 Paris, France

*To whom correspondence should be addressed at: Section on Endocrinology and Genetics, *Eunice Kennedy Shriver* National Institute of Child Health and Human Development, National Institutes of Health, 10 Center Drive, Building 10, NIH-Clinical Research Center, Room 1-3330, MSC1103, Bethesda, MD 20892, USA. Tel: +1 3014964686; Fax: +1 3014020574; Email: stratakc@mail.nih.gov

Abstract

Inactivating mutations in the Armadillo repeat-containing 5 (*ARMC5*) gene have recently been discovered in primary macronodular adrenal hyperplasia (PMAH), a cause of Cushing syndrome. Biallelic *ARMC5* inactivation in PMAH suggested that *ARMC5* may have tumor suppressor functions in the adrenal cortex. We generated and characterized a new mouse model of *Armc5* deficiency. Almost all *Armc5* knockout mice died during early embryonic development, around 6.5 and 8.5 days. Knockout embryos did not undergo gastrulation, as demonstrated by the absence of mesoderm development at E7.5. *Armc5* heterozygote mice ($Armc5^{+/-}$) developed normally but at the age of 1 year, their corticosterone levels decreased; this was associated with a decrease of protein kinase A (PKA) catalytic subunit α (Cα) expression both at the RNA and protein levels that were also seen in human patients with PMAH and *ARMC5* defects. However, this was transient, as corticosterone levels normalized later, followed by the development of hypercorticosteronemia in one-third of the mice at 18 months of age, which was associated with increases in PKA and Cα expression. Adrenocortical tissue analysis from $Armc5^{+/-}$ mice at 18 months showed an abnormal activation of the Wnt/β−catenin signaling pathway in a subset of zona fasciculata cells. These data confirm that Armc5 plays an important role in early mouse embryonic development. Our new mouse line can be used to study tissue-specific effects of Armc5. Finally, *Armc5* haploinsufficiency leads to Cushing syndrome in mice, but only later in life, and this involves PKA, its catalytic subunit Cα, and the Wnt/β−catenin pathway.

Introduction

Bilateral adrenocortical hyperplasias (BAH) may be responsible for excessive production of cortisol, aldosterone and/or androgens. Cortisol-producing BAHs lead to Cushing syndrome (CS); among them, primary pigmented micronodular adrenal disease (PPNAD) and primary macronodular adrenal hyperplasia (PMAH) are the most common types. Deregulation of the protein kinase A (PKA) pathway, which is essential for cortisol production, is associated with both of these hyperplasias (1). PKA is a heterotetramer composed of two catalytic and two regulatory subunits. In the presence of cAMP, the catalytic subunits are dissociated and phosphorylate their targets proteins, among them steroidogenic enzymes, and molecules such as *Star*.

Mouse protocol registration number: ASP#15-033
Received: April 6, 2017. **Revised:** June 2, 2017. **Accepted:** June 9, 2017

Inactivating mutations in the *PRKAR1A* gene encoding for R1α, the main regulatory subunit of PKA, is the main cause of PPNAD (2–4).

Although PMAH was initially considered as a sporadic disease, the identification of germline mutations in the Armadillo-containing 5 (ARMC5) gene on chromosome 16p in ∼40% of PMAH patients demonstrated that PMAH is in fact most frequently a hereditary disorder (5–9). *ARMC5* mutations were found at both the germline and tumor levels; they were mostly frameshift and nonsense mutations leading to ARMC5's loss of function (6), suggesting that *ARMC5* may act as a tumor suppressor gene. Interestingly, as PMAH patients usually develop several nodules, germline-independent and 'private' somatic *ARMC5* mutations were identified in each one of the lesions. In one such extreme example, we identified a single germline and 15 somatic mutations in a patient with PMAH (7). Thus, *ARMC5* mutations may be associated with extreme mutability and genetic heterogeneity of the other allele (7).

ARMC5 mutations are associated with the development of PMAH but the exact role played by *ARMC5* in the development of these adrenocortical nodules remains unknown. *ARMC5* knock down using siRNA in the adrenocortical cell-line H295R induced a reduction of cortisol secretion both in basal conditions and after forskolin-induction owing to decrease in the expression of specific steroidogenic enzymes, such as *CYP17A1*, *CYP21A2* and *MC2R* (5). This observation was in contradiction with the hypercortisolism observed in patients with PMAH. It was hypothesized that this apparent paradox could be explained by the fact that adrenal glands in PMAH patients were several fold-larger, and thus the increase in cortical mass overcompensated for the relative decrease in expression of the steroidogenic enzymes.

To better understand the role of *ARMC5* in adrenal function and tumorigenesis, we generated a new mouse model of *Armc5* inactivation, bearing *LoxP* sites, so that it can also be used for tissue-specific and other studies, if needed. *Armc5* knockout (KO) mice ($Armc5^{-/-}$) died during relatively early embryonic development, demonstrating an apparently essential role played by Armc5 during gastrulation. The Armc5 heterozygote mouse ($Armc5^{+/-}$), which replicates the genetics of patients with germline *ARMC5* inactivating mutations, developed hypocorticosteronism at least in part owing to a down-regulation of a subset of steroidogenic enzymes (*star*, *cyp11a1*, *cyp21*) at 12 months of age. However, one-third of the analyzed mice (3/9) at that age had increased corticosterone level later in life (at 18 months of age), suggesting an age-dependent and evolving role of ARMC5 in adrenocortical function.

Results

Armc5 inactivation in mice

LacZ and neomycin resistant cassettes were inserted between the exons 1 and 2 of *Armc5* gene, flanked by *LoxP* sites (Fig. 1A). $Armc5^{+/-}$ male and female were mated and as expected, mice heterozygote and homozygote, thereafter referred to as $Armc5^{+/-}$ and $Armc5^{-/-}$ (KO), respectively, were readily detected by genomic PCR (Fig. 1B). However, after genotyping at weaning, we got only 0.025% of live $Armc5^{-/-}$ mice (instead of the 25% expected) (Fig. 1C), suggesting that most of $Armc5^{-/-}$ mice died prematurely. Indeed, $Armc5^{+/-}$ females gave birth to fewer pups than $Armc5^{+/+}$ females (Supplementary Material, Fig. S1), showing that most mice died during embryonic development. However, this phenotype was not fully penetrant, as few $Armc5^{-/-}$ mice (a total of 3 $Armc5^{-/-}$ in 21 breeding pairs) survived in this mixed background (C57/BL6, 129 Sv/J and Swiss). Interestingly, at weaning, $Armc5^{-/-}$ mice were smaller and lighter than their littermates (Fig. 1D). This difference was found both in females and males and was maintained overtime even though $Armc5^{-/-}$ mice showed normal growth curves (Fig. 1E and F), but appeared to be sterile. The heterozygotes, $Armc5^{+/-}$ mice, did not show any differences in weight or length, compared with wild-type (WT), $Armc5^{+/+}$ mice (Fig. 1E and F).

Role of Armc5 during embryonic development

As it was evident that Armc5 plays an essential role during embryonic development, we analyzed Armc5 expression at E6.5, E7.5, E10.5 and E14.5 (Fig. 2). We collected $Armc5^{+/-}$ embryos from several embryonic stages and stained them for β-galactosidase as these embryos have the LacZ cassette under the control of the *Armc5* promoter. We showed that Armc5 is expressed in all the cells of embryo at the earliest stages (E6.5 and E7.5) but its expression pattern became more specific after E14.5 (Fig. 2d). Although ARMC5 is mainly a cytoplasmic protein in human adrenocortical cells (5), Armc5's expression was mostly membranous at E6.5 and E7.5 (Fig. 2A and B) and co-localized perfectly with another Armadillo protein, β – catenin (Supple Mouse protocol registration numbermentary Material, Fig. S2). This difference in expression pattern may reflect differences in pathway and/or function.

To evaluate the stage at which $Armc5^{-/-}$ embryos died, we sacrificed pregnant females through the development. The number of $Armc5^{-/-}$ embryos is still significantly lower than predicted at E13.5 (Supplementary Material, Fig. S1B) and absorptions were identified in the uterine corns (data not shown) confirming that the development of $Armc5^{-/-}$ embryos stopped before E13.5. Between E6.5 and E8.5, the number of embryos observed in $Armc5^{+/-}$ females was similar to the number of embryos from $Armc5^{+/+}$ females suggesting that $Armc5^{-/-}$ embryos were still developing at this stage. Homozygous mutant embryos lacked Armc5 protein (Fig. 3A). From E7.5, WT and mutant embryos can be identified based on their morphological differences. $Armc5^{+/+}$ and $Armc5^{+/-}$ embryos had formed mesoderm and underwent gastrulation (Fig. 3B). Mesoderm formation and gastrulation were not observed in $Armc5^{-/-}$ embryos (Fig. 3B, d, g) as demonstrated by the ubiquitous expression of E-cadherin, an endodermic marker in the latter (Fig. 3B, e, h). However, the embryonic ectoderm of the mutant embryo expressed Oct4 suggesting that the proximal-distal polarity of the embryo was established correctly (Fig. 3B, f, i).

In conclusion, complete inactivation of *Armc5* prevented gastrulation, suggesting that Armc5 plays a key role in the differentiation of the three embryonic layers, and especially the mesoderm.

Armc5 heterozygosity was associated with changes in adrenocortical morphology

To study the dynamics of Armc5 expression in adrenal development, we first carried out comparative expression analysis at various developmental stages using a β-galactosidase antibody. At E14.5 and 18.5, Armc5 is expressed only in the cortical cells as demonstrated by the absence of co-localization between Armc5 and the medullary marker, tyrosine hydroxylase (TH) (Fig. 4A). Similarly, in adult adrenal gland, Armc5 expression was found in both zona glomerulosa (ZG) and fasciculata as

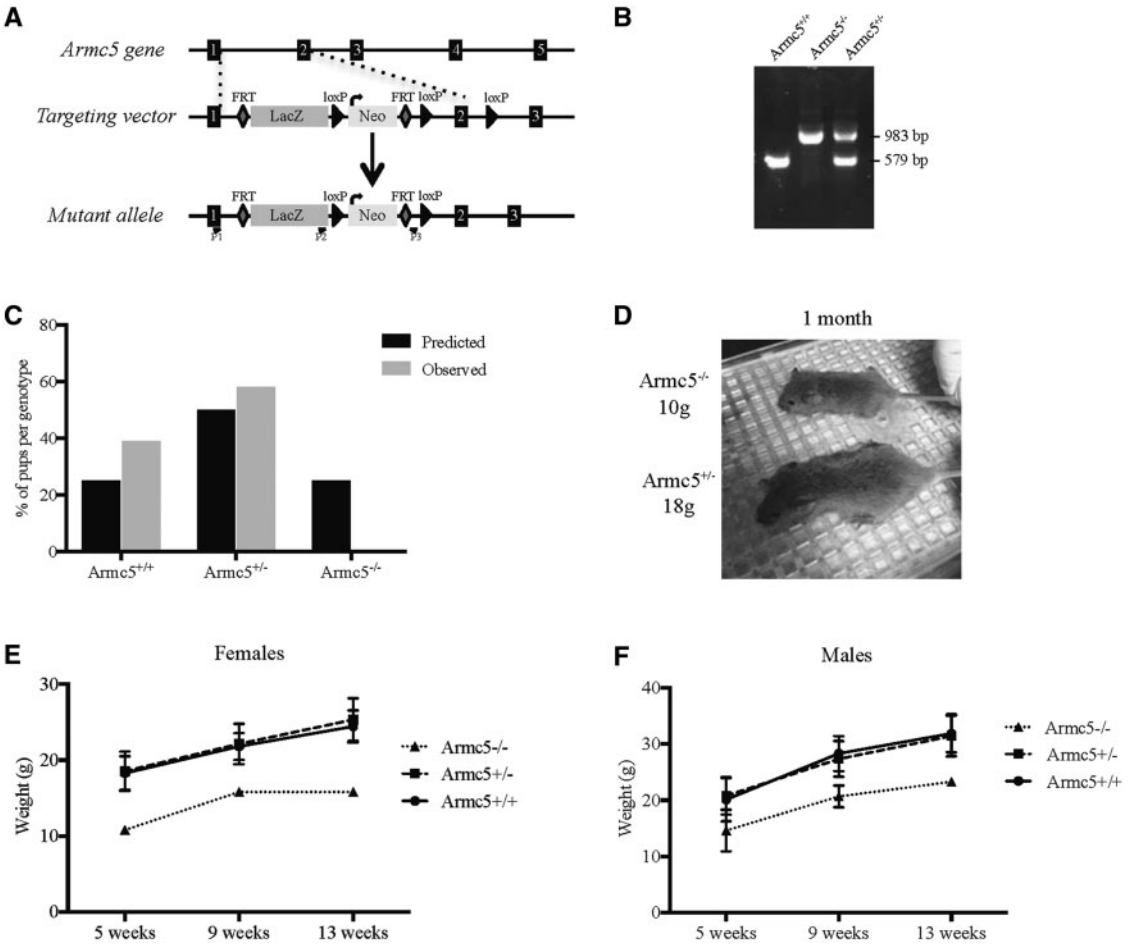

Figure 1. Knocking out *Armc5* in mouse. (**A**) Gene targeting strategy. *Armc5* exons are shown in black. In the targeting vector, LacZ and neomycin resistance gene (Neo) are inserted between the exons 1 and 2 of mouse *Armc5* gene. The location of primers used for genotyping is shown along. (**B**) PCR analysis of Armc5 locus in $Armc5^{+/+}$, $Armc5^{+/-}$ and $Armc5^{-/-}$ mice. The identity of the PCR products was confirmed by the size of the amplicon. (**C**) Only 0.025% of $Armc5^{-/-}$ embryos are still alive at weaning. The numbers of pups born from breeding between two $Armc5^{+/-}$ mice are presented in gray while the expected Mendelian proportions are in black. (**D**) $Armc5^{+/+}$ and $Armc5^{-/-}$ males at weaning. $Armc5^{-/-}$ male is clearly smaller and lighter (10 g) than its littermate (18 g). The weight of $Armc5^{+/+}$, $Armc5^{+/-}$ and $Armc5^{-/-}$ females (**E**) and males (**F**) was monitored over time. $Armc5^{-/-}$ females and males were significantly smaller than $Armc5^{+/-}$ and $Armc5^{+/+}$ littermates even though they grew without any obvious defects.

shown by colocalization with Cyp11a1 (Fig. 4B) but not in the medulla (Fig. 4A). Armc5 is then expressed in the cortical cells from the early adrenal development and its expression is maintained through time.

We then characterized the adrenals from $Armc5^{+/-}$ mice. We first evaluated Armc5 expression in $Armc5^{+/-}$ adrenals at 6-, 12- and 18-month-old females (Fig. 5A). Armc5 expression was significantly decreased in $Armc5^{+/-}$ adrenals compared with controls both in females at 6 months of age (Fig. 5A) and males at 12 months of age (Supplementary Material, Fig. S3A). We further characterized carefully the adrenal glands. At 6 months of age, adrenal morphology was similar in WT and $Armc5^{+/-}$ females (Supplementary Material, Fig. S4). However, in some mice, at 12 months of age (4/8, 50%) fibroblastic-like cells invaded the cortex originating from the capsule (Fig. 5B, arrowheads). Very eosinophilic cells with bigger cytoplasm accumulated at the corticomedullary border (Fig. 5B, dashed circle). Despite histological variability, the adrenal cortex of $Armc5^{+/-}$ mice appeared to be globally thinner but the adrenal weight was not significantly different (data not shown). At 18 months of age, there was invasion of the adrenal cortex by fibroblastic-like cells that appeared to be more round and more frequent (4/6, 66%) than previously but had a very reduced cytoplasm (Fig. 5B, arrowheads). The eosinophilic cells became more frequent (Fig. 5B, arrows) and some area at the border between the cortex and the medulla looked fibrotic (Fig. 5B, circle) suggesting that the adrenal cortex was damaged, even though the main cortical architecture was maintained.

To better investigate the adrenocortical cells in all mice, we performed electronic microscopy on 18-month-old $Armc5^{+/+}$ and $Armc5^{+/-}$ adrenals. $Armc5^{+/-}$ adrenals showed an accumulation of lipids in zona fasciculata cells (Fig. 5C, arrowheads) with disrupted mitochondrial cristae and an increase of lysosomes. At the corticomedullary border, some cells looked almost necrotic (Fig. 5C).

Armc5 heterozygosity induced first lower, and then higher, corticosterone levels

We sequentially measured serum corticosterone concentration at 2, 6, 9, 12 and 18 months in $Armc5^{+/+}$ and $Armc5^{+/-}$ mice. In agreement with the histological data suggesting a decrease in

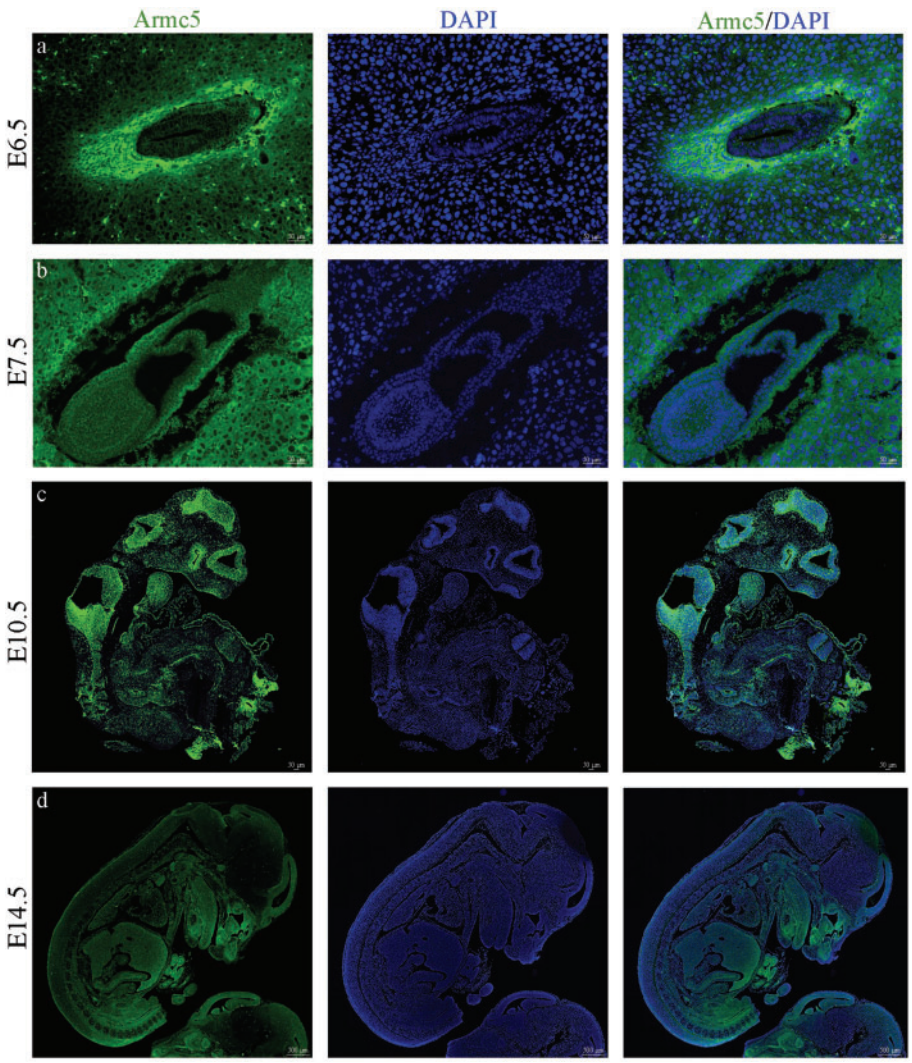

Figure 2. Armc5 expression during the embryonic development: β-galactosidase immunohistochemistry shows Armc5 expression (green) in Armc5$^{+/-}$ embryos at E6.5, E7.5, E10.5 and E14.5. DAPI (blue) is staining the nucleus of the cells.

the width of the adrenal cortex at 12 months of age, there was a 2-fold decrease in serum corticosterone concentration (Fig. 6A) associated with an increase in ACTH levels (Fig. 6B). Interestingly, serum ACTH concentrations significantly increased at 9 months of age, presumably compensating for decreased adrenal function, since corticosterone levels at the same age were normal. Indeed, dexamethasone suppressed both ACTH (data not shown) and corticosterone levels (Supplementary Material, Fig. S5). Altogether, these results demonstrated that the pituitary–adrenal axis is working properly in *Armc5*$^{+/-}$ mice, but the adrenal cortex gradually fails to produce normal corticosterone levels by 12 months of age, and this is compensated by increased ACTH levels.

Decreased corticosterone levels were in agreement with the decreases in *star*, *Cyp11a1*, *Cyp21* expression that we detected by RTqPCR (Fig. 6C) at 12 months of age. Indeed, the expression of these steroidogenic enzymes is normal at 6 months of age (Supplementary Material, Fig. S6A), and the decline was found only in *Armc5*$^{+/-}$ females. Male mice had normal corticosterone levels at 12 months of age (Supplementary Material, Fig. S3B). These data suggested that Armc5 may regulate directly or indirectly a subset of steroidogenic enzymes involved in corticosterone synthesis.

Surprisingly, corticosterone levels were significantly increased in most *Armc5*$^{+/-}$ *mice* between 12 and 18 months old (Figure 6A) in females. Despite the large variability observed at 18 months of age, 3 *Armc5*$^{+/-}$ mice had higher serum corticosterone concentration than the average of control littermates (Supplementary Material, Fig. S7). In agreement with the increases in corticosterone concentration, the expression of the steroidogenic enzymes *star*, *Cyp11a1* was normalized at 18 months, whereas *Cyp21* was now overexpressed compared with controls (Fig. 6C). Even though *Cyp11a1* expression was normal at the RNA level, Cyp11a1 protein was only expressed in a subset of fasciculata cells at 18 months of age (Fig. 6D) counter to its expression in 6 months adrenals (Supplementary Material, Fig. S6B). Similarly, Akr1b7, which is a fasciculata marker, was not expressed in all zona fasciculata cells, suggesting that at this stage, Armc5 is involved in the differentiation of the fasciculata cells.

We also tested for the expression of proopiomelanocortin (*Pomc*), 5-hydroxytryptamine receptor 1D (*Htr1d*), dopamine receptor D2 (*Drd2*), gastric inhibitory polypeptide receptor (*Gipr*), adrenergic receptor 2A (*Adra2a*), arginine vasopressin receptor 1A (*Avpr1a*), luteinizing hormone receptor (*Lhr*) and follicle

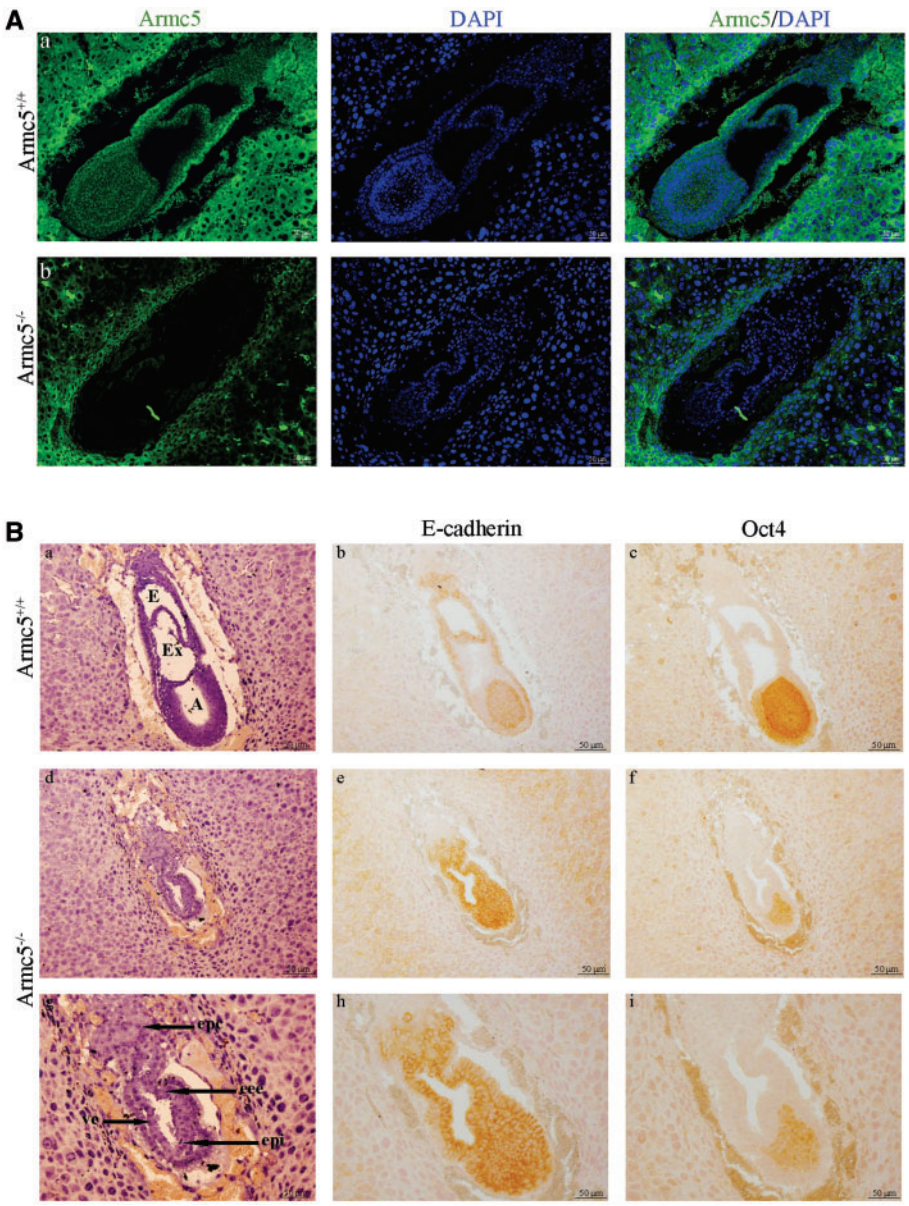

Figure 3. *Armc5*$^{-/-}$ embryos at E7.5 days of development. (**A**) Armc5 expression (green) is analyzed by immunofluorescence in *Armc5*$^{+/+}$ (a) and *Armc5*$^{-/-}$ embryos (b) at E7.5. Although Armc5 is normally expressed in the maternal tissue, *Armc5*$^{-/-}$ embryo does not express Armc5. (**B**) Hematoxylin/eosin-stained sections of *Armc5*$^{+/+}$ (a) and *Armc5*$^{-/-}$ (d, g) embryos at E7.5. E: ectoplacental cavity; Ex: exocoelom; A: amniotic cavity; Epc: ecoplacental cone; eee: extra-embryonic ectoderm; ve: visceral endoderm; epi: epiblast; M: mesoderm. Immunohistochemistry on sagittal sections with E-cadherin (b, e, h) and Oct4 (c, f, i) antibodies.

stimulating hormone receptor (*Fshr*) expression by RTqPCR on WT and *Armc5*$^{+/-}$ adrenals at 6, 12 and 18 months of age. Although no significant differences were detected at 6 months, *Adra2a*, *Avpr1a* and *Htr1d* expression was significantly increased at 12 months of age (Supplementary Material, Fig. S8). This upregulation was, however, again transient and the expression of these molecules was similar across genotypes at 18 months of age (Supplementary Material, Fig. S8C).

Altogether these results suggested that Armc5 is involved in the regulation of zona fasciculata function across ages. Armc5 deficiency affected corticosterone production at least, in part, through the regulation of a subset of steroidogenic enzymes. This effect appears to be time-dependent and maybe influenced by aging and does not appear to be strongly linked to aberrant ectopic receptor expression.

Armc5 and the PKA pathway in mice and humans

The expression of the three genes that are critical for steroidogenesis and were significantly down-regulated in *Armc5*$^{+/-}$ adrenal glands, *star*, *Cyp11a1* and *Cyp21*, is controlled by the steroidogenic factor 1, *Sf1* (10). Interestingly, *Sf1* expression was significantly decreased specifically in 12 months old *Armc5*$^{+/-}$ adrenals (Fig. 7A) whereas its expression was not modified at 6 months (Supplementary Material, Fig. S6C). As *Sf1* is known to be a PKA pathway-target gene, we analyzed the expression of the PKA subunits by RTqPCR (Fig. 7B). Only the expression of the catalytic subunit α, *Pkraca* was significantly decreased (Fig. 7B) at 12 months of age, confirmed also at the protein level (Fig. 7C, left panel-D). However, the total PKA activity was not significantly modified in *Armc5*$^{+/-}$ adrenals neither at baseline nor

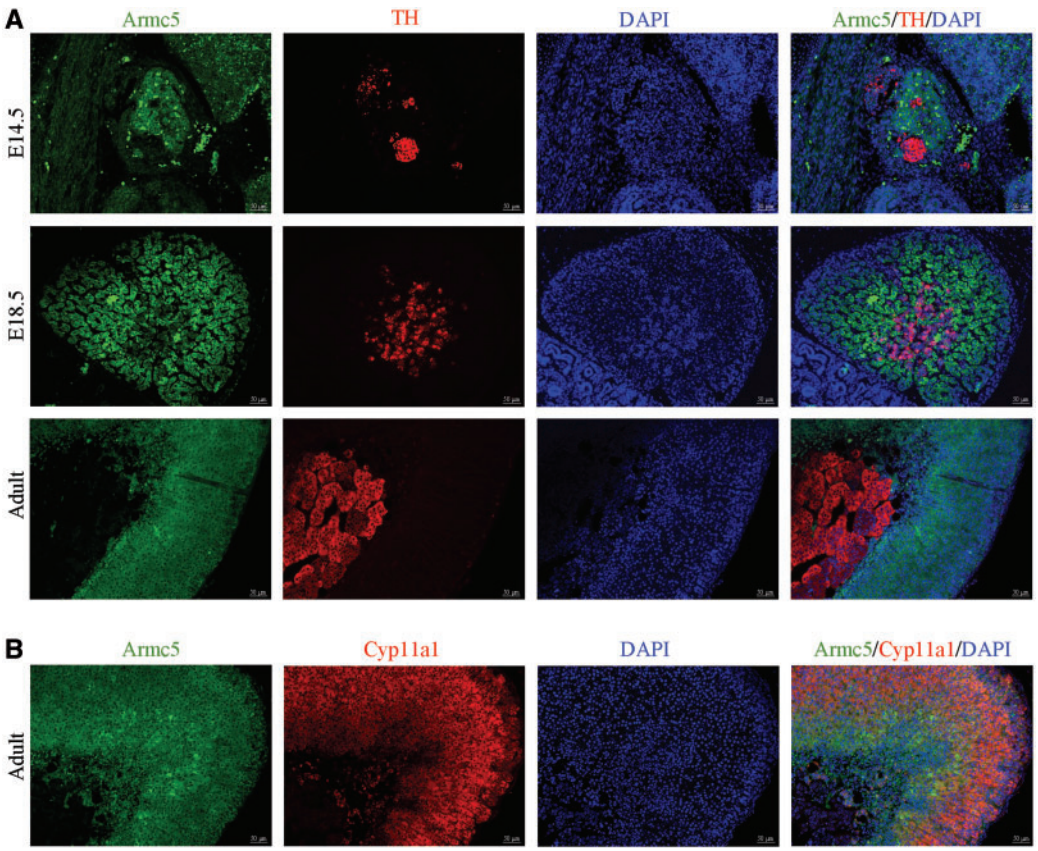

Figure 4. Armc5 is expressed exclusively in the adrenal cortex during embryonic development. (**A**) Immunofluorescence of Armc5 (green) and TH (red) shows that Armc5 is not expressed in TH-positive cells at 14.5, 18.5 days of development and adult adrenal. (**B**) Immunofluorescence of Armc5 (green) and Cyp11a1 (red) demonstrates that Armc5 is expressed in adrenocortical cells.

after cAMP stimulation (Fig. 7E). Conversely, Cα protein was increased in *Armc5*$^{+/-}$ adrenals at 18 months of age (Fig. 7C, right panel-D), which was associated with an increase in PKA activity at basal conditions (Fig. 7E).

These data showed that Armc5 acts at least in part through PKA to regulate adrenocortical steroidogenesis and function in an age-dependent manner. Accordingly, no difference was found at 6 months old (Supplementary Material, Fig. S6D–G) when the corticosterone level was not modified.

To determine if the effect of Armc5 on the PKA pathway is conserved in humans, we analyzed Cα and R1α protein expression by western blot in PMAH samples from patients with and without *ARMC5* mutations (Fig. 7F). Cα expression tended to decrease in PMAH with *ARMC5* mutations compared with PMAH without mutations, which is associated with a significant decreased of PKA activity in basal conditions (Fig. 7G) but not after cAMP induction.

These data confirmed that in humans with PMAH, too, ARMC5 interacts with PKA and regulates *PRKACA* expression.

Armc5 and mouse adrenal ZG

Serum aldosterone concentration was not modified in *Armc5*$^{+/-}$ mice neither at 6, 12 and 18 months old (Supplementary Material, Fig. S9). However, to determine if *Armc5* heterozygosity altered ZG structure and/or differentiation, we analyzed β−catenin expression by immunohistochemistry (Fig. 8A). β-catenin was accumulated in the cytoplasm and slightly in the nucleus of the glomerulosa cells demonstrating that the Wnt/β-catenin pathway was activated. This same pattern was found in WT *Armc5*$^{+/+}$ and *Armc5*$^{+/-}$ mice at 12 months of age but the ZG in *Armc5*$^{+/-}$ mice was disrupted owing to the accumulation of fibroblastic-like cells, which were not expressing β-catenin (Fig. 8A). However, at 18 months of age, β-catenin accumulated in the cytoplasm of some cells that were abnormally located in zona fasciculata suggesting that β-catenin was activated in these cells (Fig. 8A, arrowheads). Accordingly, the expression of three Wnt/β-catenin targets genes, *Axin2*, *Lef1* and *CyclinD1* was significantly increased in *Armc5*$^{+/-}$ adrenals (Fig. 8B and D).

In conclusion, *Armc5* haploinsufficiency appears to leads to Wnt/β-catenin activation in the aging adrenal cortex.

Discussion

Although it has been shown that *ARMC5* mutations are associated with ∼40% of cases with PMAH, the molecular mechanisms involving ARMC5 in the development of adrenal macronodular hyperplasia remain unknown. In the current study, we report the adrenal characterization of a newly created mouse model that is heterozygote for *Armc5*.

Our analysis demonstrated that Armc5 regulates steroidogenesis, at least in part, through the PKA pathway. Indeed, at 12 months old, *Armc5*$^{+/-}$ mice showed down-regulation of the PKA catalytic subunit Cα both at RNA and protein levels, and this was associated with a reduction of expression of steroidogenic molecules regulated by PKA such as *star*, *Cyp11a1*, *Cyp21* leading

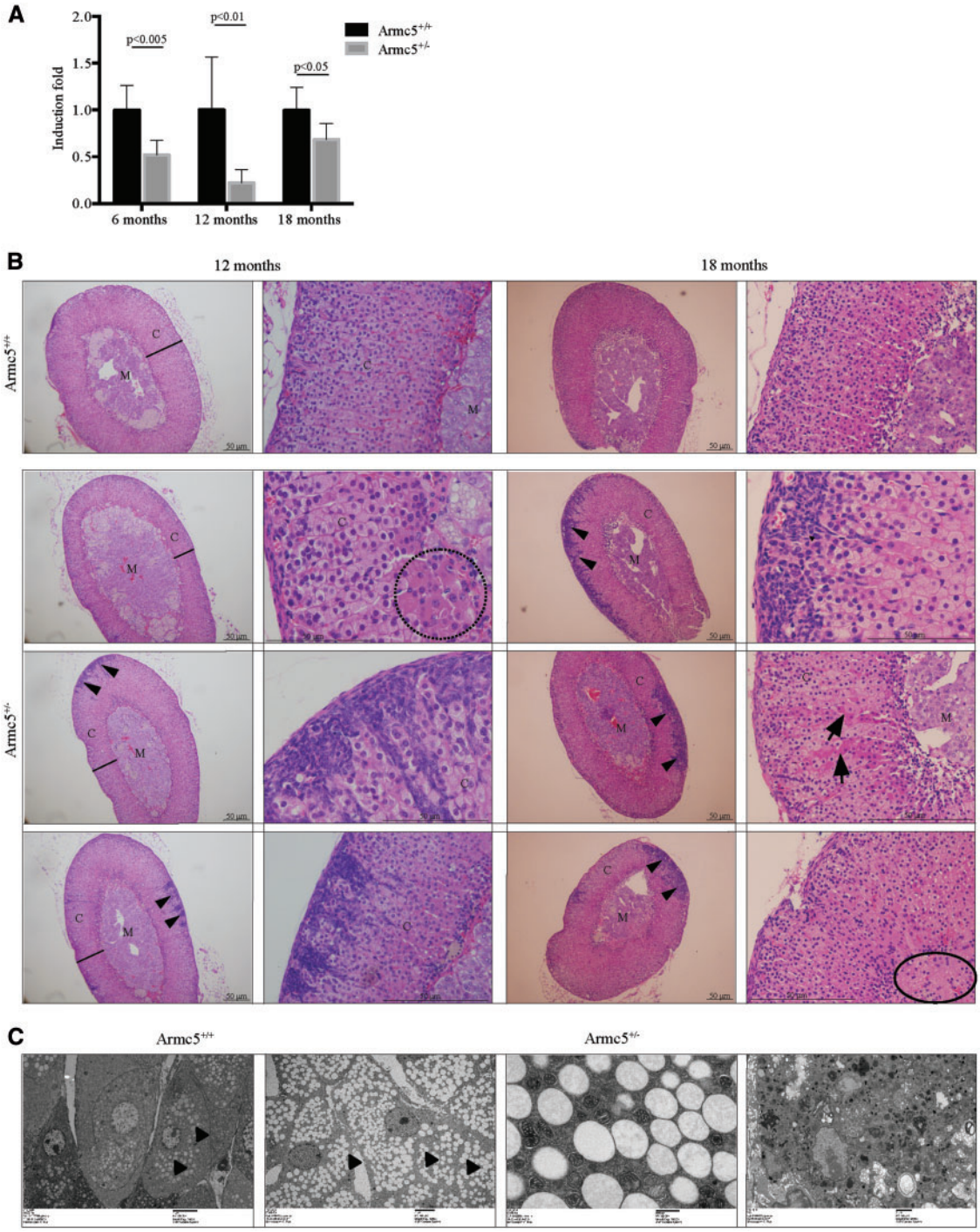

Figure 5. Histology of *Armc5*$^{+/-}$ adrenals from female mice. (**A**) Armc5 expression is significantly decreased in *Armc5*$^{+/-}$ adrenals at 6, 12 and 18 months. (**B**) Histology of *Armc5*$^{+/+}$ and *Armc5*$^{+/-}$ adrenals at 12 and 18 months. C: Cortex; M: Medulla. A black line indicated the width of the cortex. Arrowhead shows the fibroblastic-like cells. Dashed circles indicate cells with different histological features. Full circles show the fibrotic area (**C**) Electronic microscopy images of fasciculata cells from *Armc5*$^{+/+}$ and *Armc5*$^{+/-}$ adrenals. Arrowheads indicate the lipids whereas arrows show the 'dark mitochondria'.

to hypocorticosteronemia. These results were surprising knowing that *ARMC5* mutations are found in patients with CS, but it is consistent with the decreases in cortisol production both at baseline and after forskolin induction, that was observed in the human adrenocortical cancer cell line, H295R after ARMC5-knockdown (5). Accordingly, we showed that PKA activity was significantly decreased in patients with PMAH with ARMC5-inactivating mutations compared with the group of patients without mutations. Altogether, these data demonstrate that hypersecretion of glucocorticoids in PMAH is a later event, induced perhaps by a complex series of pathophysiological and/or molecular events. This does not appear to depend on ectopic hormone receptor expression, a well described phenomenon in humans with PMAH.

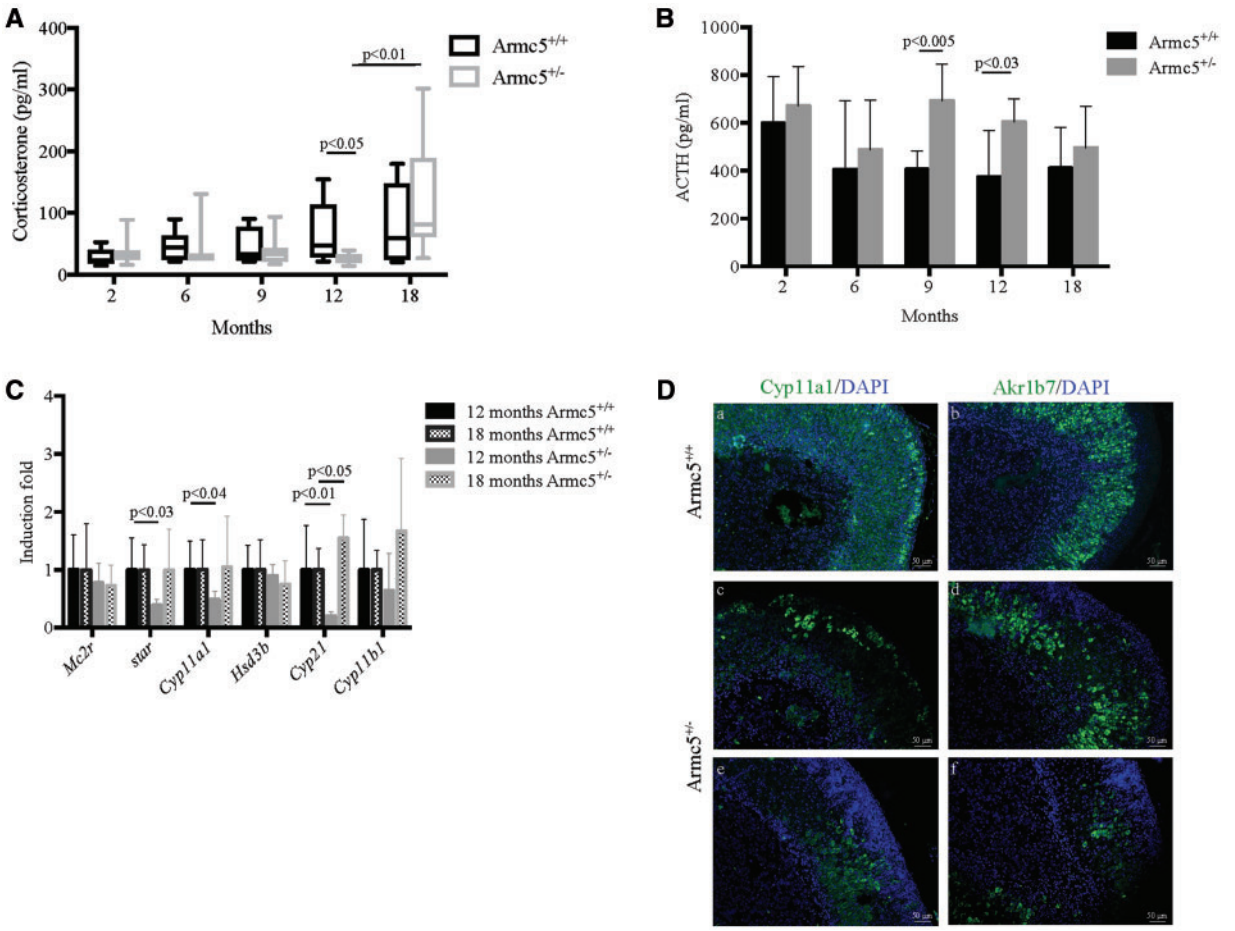

Figure 6. Heterozygosity for *Armc5* deficiency leads to a hypocorticosteronemia at 12 months old. (**A**) Serum corticosterone concentration is significantly decreased in *Armc5*$^{+/-}$ mice at 12 months old but increased at 18 months. Bars represent the median corticosterone level of at least six individual adrenals ± standard deviation. (**B**) Serum ACTH concentration is significantly increased in 9 and 12 months old mice. Bars represent the mean ACTH level of at least six individual adrenals ± standard deviation. (**C**) *star*, *Cyp11a1* and *Cyp21* expression is significantly decreased in *Armc5*$^{+/-}$ adrenals. *Mc2r*, *star*, *Cyp11a1*, *Hsd3b*, *Cyp21* and *Cyp11b1* expression was analyzed by RTqPCR on mRNA from 12 and 18 months old *Armc5*$^{+/+}$ and *Armc5*$^{+/-}$ adrenals. Bars represent the induction fold of at least six individual adrenals ± standard deviation. *P*-value was calculated using Student's *t*-test. (**D**) Immunofluorescence for Cyp11a1 (a, c, d, green) and Akr1b7 (b, d, e, green) in adrenals from 18-month-old mice; DAPI stained the nuclei.

PMAH is characterized by the development of adrenocortical nodules over time (5). However, the adrenals from *Armc5*$^{+/-}$ mice did not grow any adrenocortical tumors, suggesting that *Armc5* haploinsufficiency is not sufficient to induce the formation of large growing lesions. Accordingly, the *Armc5* KO mice, whose analysis was only recently reported, were not found to develop tumors either (11). On the other hand, our analysis showed the presence of lesions that were microscopic, associated with altered mitochondrial structure and number, and were associated with increased steroid hormone production, all features of human PMAH owing to *ARMC5* defects.

There was no difference in serum corticosterone concentration between *Armc5*$^{+/+}$ and *Armc5*$^{+/-}$ mice before 12 months of age. At this age, in fact, the corticosterone concentration increased in WT (*Armc5*$^{+/+}$), but not in *Armc5*$^{+/-}$ mice. This suggests that *Armc5*$^{+/-}$ mice did not produce corticosterone as readily as WT mice, which is consistent with their higher ACTH levels observed at both 9 and 12 months. Interestingly, the corticosterone elevation observed in *Armc5*$^{+/-}$ mice as they aged, was similar to the cortisol increases seen in humans with PMAH as they grow older (12). This suggests that ARMC5's role in glucocorticoid synthesis may be increased in the aging adrenal, which could be one of the reasons why PMAH is most frequently diagnosed in older patients (13). It would be interesting to determine if before developing PMAH, PMAH patients have low cortisol concentration. This is now possible to study as more and more families are identified with PMAH owing to *ARMC5* mutations that are present across generations but do not lead to CS in all carriers.

Thus, a subset of *Armc5*$^{+/-}$ mice (30%) had a significant increase in their corticosterone levels compared with WT mice at 18 months of age. There was no overall significant difference in the serum corticosterone concentration between the two groups of mice at the same age. Again, this is reminiscent of the human situation: in the most recent study, only 30% of patients carrying a pathogenic *ARMC5*-inactivating mutation developed CS (8).

In this study, we demonstrated that *Armc5* KO mice died during early embryonic development, which is in agreement with the results recently published by Hu *et al.* (11). So, now, two different genetic constructs leading to inactivation of the mouse *Armc5* gene, resulted in embryonic lethality confirming the essential role of this gene during development. In our mouse model, we were able to demonstrate that *Armc5*$^{-/-}$ embryos did not undergo gastrulation. Another well-known Armadillo

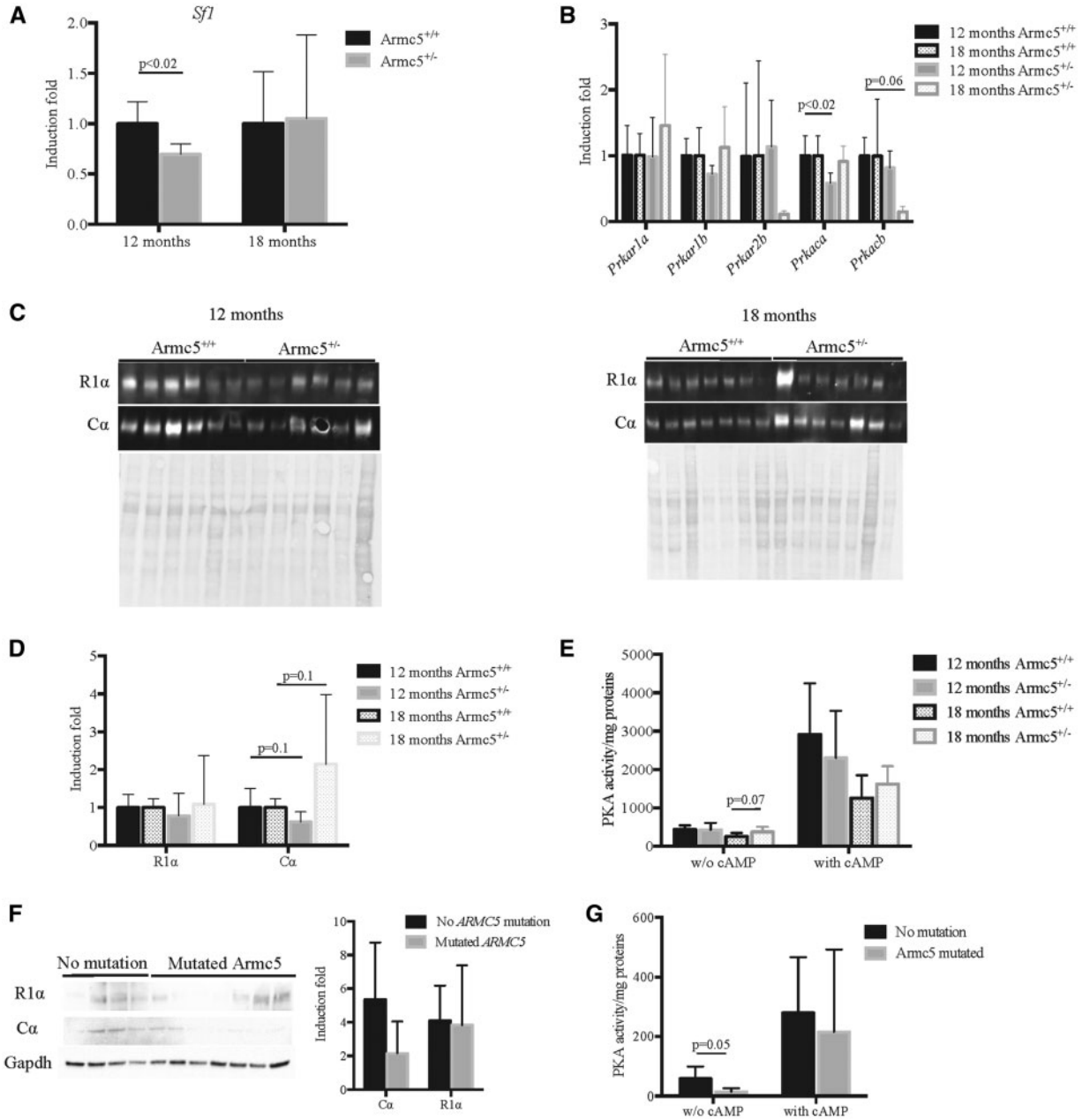

Figure 7. Heterozygosity for ARMC5 deficiency in mice and humans alters the PKA pathway. (**A**) *Sf1* expression is significantly decreased in *Armc5*$^{+/-}$ adrenals at 12 months only. (**B**) *Prkaca* expression is significantly decreased in Armc5$^{+/-}$ adrenals; *Prkar1a*, *Prkar1b*, *Prkar2b*, *Prkacb* and *Prkaca* expression was analyzed by RTqPCR on mRNA from 12 and 18 months old Armc5$^{+/+}$ and Armc5$^{+/-}$ adrenals. Bars represent the induction fold quantification at least six individual adrenals ± standard deviation. *P*-value was calculated using Student's *t*-test. (**C**) Cα protein accumulation is decreased in Armc5$^{+/-}$ adrenals at 12 months and increased at 18 months. Western blot analysis was done on at least six adrenals per genotype. (**D**) Western blot quantification. (**E**) PKA activity is increased in *Armc5*$^{+/-}$ adrenals at basal condition at 18 months. Bars represent the mean PKA activity on at least six individual adrenals ± standard deviation. *P*-value was calculated using Student's *t*-test. (**F**) Cα expression is decreased in the nodules of human patients with PMAH carrying *ARMC5* mutations. Western blot analysis of Cα, R1α and GAPDH expression on PMAH with and without *ARMC5* mutations. Bars represent the mean in at least four individuals per conditions ± standard deviation. (**G**) PKA activity is decreased in nodules with *ARMC5* mutations in basal conditions only. Bars represent the mean PKA activity on at least four individual adrenals ± standard deviation. *P*-value was calculated using Student's *t*-test.

protein, β-catenin, is essential for the gastrulation of the developing embryo (14,15) and interestingly, Armc5 and β-catenin expression co-localized in membranes in E6.5 and E7.5 embryos. It has been demonstrated that β-catenin acts mainly through its central role in Wnt/β-catenin pathway in the gastrulation-stage embryo (16) suggesting that Armc5 plays a role in this pathway, too.

Wnt/β-catenin pathway plays an essential role in adrenal cortex homeostasis and tumorigenesis (17–20). β-Catenin nucleo-cytoplasmic accumulation, is a sign of Wnt/β-catenin pathway activation, is well regulated and limited to the ZG (19). Indeed, constitutive activation of β-catenin has been described in adrenocortical tumors and carcinomas (17,18,20). Mice with constitutive activation of β-catenin specifically in the adrenal

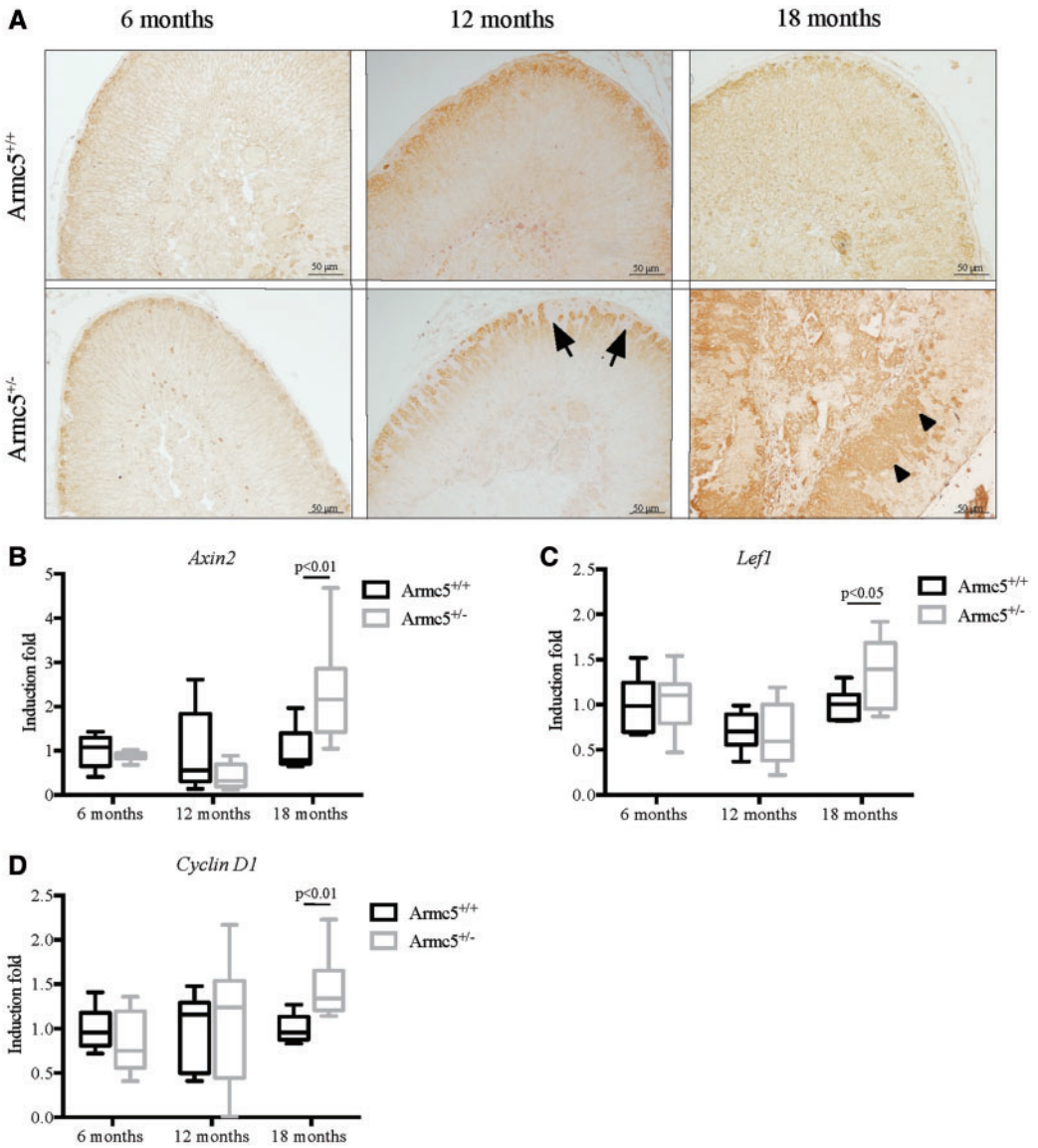

Figure 8. Wnt/β–catenin pathway analysis in Armc5$^{+/-}$ adrenals. (**A**) Immunohistochemical analysis of β-catenin shows a normal expression in the zona glomerulosa (ZG) of Armc5$^{+/-}$ adrenals. However, the ZG is invaded by the fibroblastic like cells (arrows) that did not express β-catenin. (**B**) The β-catenin target genes *Axin2*, *Lef1* and *CyclinD1* are significantly increased in *Armc5*$^{+/-}$ adrenals at 18 months old. Their expression was analyzed by RTqPCR on mRNA from 12 and 18-month-old *Armc5*$^{+/+}$ and *Armc5*$^{+/-}$ adrenals. Bars represent the induction fold of at least six individual adrenals ± standard deviation. *P*-value was calculated using Student's *t*-test.

cortex develop adrenocortical hyperplasia, which, in some cases, progressed to carcinoma. In the mice described here, although, at 12 months, Wnt/βcatenin pathway was activated only in the ZG, β-catenin was abnormally accumulated in the nuclear and/or cytoplasm of cells located in the zona fasciculata (in *Armc5*$^{+/-}$ females, at 18 months of age). The abnormal activation of Wnt/β-catenin was confirmed by the overexpression of two target genes, *Axin2* and *Lef1* suggesting that Armc5 heterozygosity leads to Wnt/β-catenin activation in aging mice. The involvement of the Wnt/β-catenin pathway in the development of PMAH has been suggested by transcriptomic and micro-RNA studies (21,22) but no mutations have been identified in the *CTNNB1* gene encoding for β-catenin in PMAH (23) unlike in PPNAD (24). Our results demonstrate that *Armc5* mutations may activate the Wnt/β-catenin pathway over time in the aging adrenal. The mechanisms involving the dual role of Armc5 and β-catenin at two different stages of life, in embryonic development and in aging remain unclear.

In 2017, Hu *et al.* showed that Armc5 is involved in T-cell immune response through an important role for T-cell proliferation and differentiation (11) demonstrating that ARMC5's function is not limited to the adrenal cortex. Indeed, cases of PMAH associated with meningioma have been described in the literature (24,25). In one of the studies (25), the authors found a germline *ARMC5* mutation (p.A110fs*9) associated with PMAH. One of the patients also developed a meningioma and a pancreatic tumor that were both sequenced for the *ARMC5* gene; a somatic *ARMC5* mutation was found in the meningioma (p.R502fs) resulting in complete inactivation of the gene in this tissue, but not in the pancreatic tumor. As ARMC5 is ubiquitously expressed (26), and quite highly expressed in the nervous and endocrine systems, further characterization of these mice may

lead to the identification of additional roles of ARMC5 in physiology and pathology.

In conclusion, we generated a new mouse model that carries a *LoxP* site and can be used for tissue-specific and other studies. We also analyzed mice that were heterozygotes for *Armc5* deficiency up to 18 months of age and studied their adrenal function. We showed that *Armc5* haploinsufficiency leads to abnormal adrenocortical steroidogenesis, involving in particular the PKA pathway, and ultimately, constitutive activation of Wnt/β-catenin signaling in at least a few cortical cells. Eventually, a subset of these mice developed hypercorticosteronemia, reminiscent of the development of PMAH in older humans with *ARMC5* mutations. It remains to be seen whether younger patients with *ARMC5*-inactivating mutations have ACTH-compensated hypocorticolemia when they are younger, like *Armc5*$^{+/-}$ mice.

Materials and Methods

Generation of a new mouse model for Armc5 deficiency

Armc5 KO mice have been generated using the homologous recombination. The plasmid harboring the LacZ and neomycin resistance cassettes between the exons 1 and 2 of the mouse *Armc5* gene was purchased from the European Conditional Mouse Mutagenesis (EUCOMM). Mouse embryonic stem cells (mES) were electroporated with Armc5 construct and selected for antibiotic resistance. The mES clones were screened by PCR using the following primers: Armc5_WT_F TCATTGCCTG TCCTGTATCTCA, Armc5_LacZ_F GCCTGCTTGCCGAATATCAT and Armc5_WT_R AGCAAGAATGTGGCAAACGT. Three positive clones were injected in mouse blastocytes and reimplanted in females in pseudo-gestation. The chimeras were crossed with WT mice to check the germinal transmission of the mutant allele and the progenies were genotyped by PCR using the primers described above. *Armc5* mice were kept in a mixed background C57/BL6, 129 Sv/J and Swiss genetic background to mimic the human condition. Use of heterozygote breeding pairs enabled the generation of the *Armc5*$^{+/+}$, *Armc5*$^{+/-}$ and *Armc5*$^{-/-}$ littermates used in the study. Both male and female mice at 12 months old were sacrificed for the RNA, protein, blood collection and dexamethasone test (27). Procedures were approved by and in accordance with the *Eunice Kennedy Shriver* National Institute for Child Health and Human Development Institutional Animal Care and Use Committee. Mice were euthanized by CO_2. Blood was collected by intracardiac puncture.

Patients and PMAH tumors

All the patients signed a consent form. The research protocol (2000-CH-0160) was approved by the Institutional Review Boards of the *Eunice Kennedy Shriver* National Institute of Child Health and Human Development (until 2010) and Diabetes and Digestive and Kidney Diseases (2010 to the present), National Institutes of Health. The germline and tumor DNA were sequenced for *ARMC5*; part of this cohort has been previously published (7,28). We classified tumors in two groups based on patients' *ARMC5* mutational status. Tumors from patients with *ARMC5* mutations had both germline and somatic *ARMC5* mutations, whereas the group without *ARMC5* mutations had neither germline nor somatic *ARMC5* mutations. Proteins were extracted from macronodules of these patients (see Western blot section).

Tissue and serum collection

Mice were sacrificed by slow replacement of air with CO_2 followed by cervical dislocation. Trunk blood was collected by intracardiac puncture and placed in serum separator tubes (365956, BD microtainer). After centrifugation (4500*g*, 3 min, 4°C), serum was stored at −80°C. Collected tissues were snap frozen on dry ice and stored at −80°C until use.

Reverse transcription PCR

Total RNA was extracted from frozen adrenals using trizol (15596-018, Life Technologies) according to the manufacturer's instructions. Five hundred nanograms of RNA were reverse transcribed using the superscript III first strand synthesis supermix (11752050, ThermoFischer). Two microliters of 1/20th dilution of cDNA were used by quantitative PCR reaction. This was conducted with either Taqman probes or specific primers (see below). Each reaction was performed in duplicate in a final volume of 15 µl with 7.5 µl of Taqman Fast advanced mastermix (4444963, Life Technologies) or SYBR green mix (4309155, Applied Biosystems) and 0.75 µl of the probes or 0.75 µl of each primers. Results were expressed as induction fold calculated using $\Delta\Delta C_T$ method. All measurements were normalized to a housekeeper gene and represent the mean value of at least six adrenals per genotype ± standard deviation. Statistical analysis was performed with Student's *t*-test when results followed a normal distribution. Taqman Gene expression assays probes used in this study were as follows: Mm00490735_m1 (*cyp11a1*), Mm01159156_g1 (*hsd3b7*), Mm00441558_m1 (*star*), Mm999 99915_g1 (*gapdh*), Mm01262510_m1 (*mc2r*), Mm00496060 (*Sf1*), Mm00435909_m1 (*Prkar1b*), Mm00660092_m1 (*Prkaca*), Mm0131 2555_m1 (*Prkacb*) and Mm01293022_m1 (*Prkar2b*).

Primers that were used in this study were as follows: *Axin2*_cDNA_F GCAGGAGCCTCACCCTTC, *Axin2*_cDNA_R TGCC AGTTTCTTTGGCTCTT, Mm_*Lef1cDNA*_F TACCACGACAAGGCCA GAG, Mm_*Lef1cDNA*_R GGTGGAGAAAGGGACCCATT, Mm_*CycD 1cDNA*_F GCATGTTCGTGGCCTCTAAG, Mm_*CycD1cDNA*_R GTC TGCTTGTTCTCATCCGC, Mm_*Cyp11b1*_F TGTATCGAGAGCTGGC AGAG, Mm_*Cyp11b1*_R AGTTCCATTGAGTTAGCCTGGA.

Immunohistochemistry and immunofluorescence

Adrenals and embryos were fixed in 4% paraformaldehyde (PFA) for 24 h at 4°C, rinsed three times in PBS for 5 min, transferred in 70% ethanol. Fixed tissues were dehydrated, paraffinized and sectioned by Histoserv Inc. (Germantown, MD, USA). Hematoxylin & eosin staining (H&E) was performed by Histoserv. Five micrograms, thick sections were deparaffinized in Histoclear (HS-202, National diagnostics) and rehydrated using ethanol gradient. After the epitope retrieval in Vector Antigen Retrieval Solution (H3300, Vector Labs) at 95°C, ARMC5 antibody (NBP1-94024, Novus, USA), β-catenin (610153, BD Biosciences), E-cadherin (3195, Cell Signaling), Oct4 (2840, Cell signaling), Cyp11a1 (abs236, Millipore), Dab2 (610464, BD Transduction), TH (22941, ImmunoStar Inc.), β-galactosidase (ab9361, Abcam, Cambridge, UK), Akr1b7 (sc-27763, Santa Cruz) was incubated overnight at 4°C. The primary antibody was detected using the appropriate secondary antibody coupled to biotin (Jackson ImmunoResearch Laboratory) following by a streptavidin-HRP amplification (016-030-084, Jackson ImmunoResearch Laboratory). The HRP activity was detected with 3,3'-diaminobenzidine tetrahydrochloride (DAB) (SK-4105,

Vector Labs). The slides were counterstained with hematoxylin (K8008, Dako).

Electronic microscopy

Mice were transcardially perfused fixed in with 2.5% glutaraldehyde, made in 30 mM HEPES buffer, pH 7.4. Excised adrenal glands were cut into 1 mm cubes and left to post fix overnight in the same fixative in a glass vial overnight at room temperature. The tissue samples were then rinsed in 0.1 M sodium cacodylate buffer, post-fixed in 0.25% osmium tetroxide, made in 0.1 M sodium cacodylate buffer, for 30 min at room temperature. Next, the samples were rinsed in 0.1 M sodium cacodylate buffer, then incubated in 1% tannic acid made in 0.1 M sodium cacodylate buffer for 30 min at room temperature, followed by a short rinse in 0.1 M sodium cacodylate buffer. Samples were rinsed in 50 mM sodium acetate buffer, and then incubated in 50 mM uranyl acetate made in sodium acetate buffer for 30 min at room temperature. Samples were dehydrated in increasing concentrations of ETOH. A 1:1 mixture of propylene oxide and Embed-812 resin (Electron Microscopy Sciences, Hatfield, PA, USA) was allowed to infiltrate the samples overnight. Next, the samples were transferred to 70% Embed-812 resin, diluted with propylene oxide and left overnight to infiltrate. After several 100% fresh Embed-812 resin exchanges, samples were embedded in fresh Embed-812 resin and polymerized in a vacuum oven set at 60°C for 24 h. Thin sections were cut on a Leica EM-UC7 Ultramicrotome (90 nm). Thin sections were picked up and placed on 200 mesh cooper grids and post-stained with lead citrate. Imaging was accomplished using a JEOL-1400 Transmission Electron Microscope operating at 80 kV and an AMT BioSprint 29 camera.

Western blot

Frozen adrenals and PMAH tumors were homogenized in RIPA buffer [50 mM Tris–HCl, pH 7.4, 150 mM NaCl, 1% Triton X-100, 0.5% Na-deoxycholate, 1 mM EDTA, 10 mM NaF, protease and phosphatase inhibitors (EMD Biosciences)]. After centrifugation, the total protein concentration was determined using Pierce BCA assay (23225, ThermoFischer). Forty nanograms of total proteins was separated on a 4–10% SDS Page gradient and transferred onto nitrocellulose membrane. Proteins were detected with an antibody targeting to PRKACA (sc48412, 1/1000, Santa Cruz) and PRKAR1A (clone, 1/500, BD Biosciences), which were in turn, recognized by Alexa 564-coupled anti-mouse. Expression was normalized to Red Ponceau staining and signals were quantified with Image lab (BioRad).

PKA activity

Frozen adrenals and PMAH tumors were homogenized in lysis buffer (20 mM Tris, pH 7.5, 0.1 mM sodium EDTA, 1 mM DTT, PMSF). After centrifugation, 10 µl protein lysate and the reaction mixture containing 50 mM Tris–HCl, 10 mM $MgCl_2$, 1 mM dithiothreitol, 25 µM kemptide and 25 µl [γ-32P]ATP (0.1 µCi/nmol) with or without 5 µM cAMP. After incubation, 10 µl of mixture reaction was spotted onto 0.23-mm phosphocellulose (Whatman P81) discs and washed three times in 0.5% phosphoric acid (438081, Sigma-Aldrich). Filters were air dried and measured by liquid scintillation counter.

Biochemical measurements

ELISA kits were used to measure plasmatic corticosterone (55-CORMS-E01, ALPCO Diagnostics), ACTH (KT-6010, KAMIYA) and aldosterone (ADI-900-173, Enzo Life Sciences) concentration.

Statistical analysis

Data were reported as mean ± standard deviation; relative changes were described as an induction fold. All data distributions were assessed for approximate normality. Continuous data were compared between two independent groups using *t* tests using Graphpad Prism (Graphpad, San Diego).

Supplementary Material

Supplementary Material is available at *HMG* online.

Acknowledgements

This work was supported by the Intramural Research Program of the *Eunice Kennedy Shriver* National Institute of Child Health and Human Development (NICHD). The authors are indebted to the NICHD's cores of transgenic mouse development (Dr Alex Grinberg) and imaging and electron microscopy [Mr Louis (Chip) Dye and Dr Vincent Schram]. Dr Stephanie Espiard was supported by a grant by INSERM, Paris France; this work was part of her graduate thesis at INSERM U 1016, CNRS UMR8104, Université Paris Descartes (http://cochin.inserm.fr/la_recherche/departements/emc/equipe-bertherat).

Conflict of Interest statement. None declared.

Funding

This work was funded by the intramural research program, NICHD, NIH.

References

1. Stratakis, C.A. (2013) cAMP/PKA signaling defects in tumors: genetics and tissue-specific pluripotential cell-derived lesions in human and mouse. *Mol. Cell. Endocrinol.*, **371**, 208–220.
2. Almeida, M.Q. and Stratakis, C.A. (2011) How does cAMP/protein kinase A signaling lead to tumors in the adrenal cortex and other tissues? *Mol. Cell. Endocrinol.*, **336**, 162–168.
3. Kirschner, L.S., Carney, J.A., Pack, S.D., Taymans, S.E., Giatzakis, C., Cho, Y.S., Cho-Chung, Y.S., Stratakis, C.A. (2000) Mutations of the gene encoding the protein kinase A type I-alpha regulatory subunit in patients with the Carney Complex. *Nat. Genet.*, **26**, 89–92.
4. Kirschner, L.S., Sandrini, F., Monbo, J., Lin, J.P., Carney, J.A. and Stratakis, C.A. (2000) Genetic heterogeneity and spectrum of mutations of the PRKAR1A gene in patients with the carney complex. *Hum. Mol. Genet.*, **9**, 3037–3046.
5. Assie, G., Libe, R., Espiard, S., Rizk-Rabin, M., Guimier, A., Luscap, W., Barreau, O., Lefevre, L., Sibony, M., Guignat, L. *et al.* (2013) ARMC5 mutations in macronodular adrenal hyperplasia with Cushing's syndrome. *New Engl. J. Med.*, **369**, 2105–2114.
6. Drougat, L., Omeiri, H., Lefevre, L. and Ragazzon, B. (2015) Novel insights into the genetics and pathophysiology of adrenocortical tumors. *Front. Endocrinol.*, **6**, 96.

7. Correa, R., Zilbermint, M., Berthon, A., Espiard, S., Batsis, M., Papadakis, G.Z., Xekouki, P., Lodish, M.B., Bertherat, J., Faucz, F.R. *et al.* (2015) The ARMC5 gene shows extensive genetic variance in primary macronodular adrenocortical hyperplasia. *Eur. J. Endocrinol.*, **173**, 435–440.
8. Espiard, S., Drougat, L., Libe, R., Assie, G., Perlemoine, K., Guignat, L., Barrande, G., Brucker-Davis, F., Doullay, F., Lopez, S. *et al.* (2015) ARMC5 mutations in a large cohort of primary macronodular adrenal hyperplasia: clinical and functional consequences. *J. Clin. Endocrinol. Metab.*, **100**, E926–E935.
9. Gagliardi, L., Schreiber, A.W., Hahn, C.N., Feng, J., Cranston, T., Boon, H., Hotu, C., Oftedal, B.E., Cutfield, R., Adelson, D.L. *et al.* (2014) Armc5 mutations are common in familial bilateral macronodular adrenal hyperplasia. *J. Clin. Endocrinol. Metab.*, **99**, E1784–1792.
10. Val, P., Lefrancois-Martinez, A.M., Veyssiere, G. and Martinez, A. (2003) SF-1 a key player in the development and differentiation of steroidogenic tissues. *Nucl. Recept.*, **1**, 8.
11. Hu, Y., Lao, L., Mao, J., Jin, W., Luo, H., Charpentier, T., Qi, S., Peng, J., Hu, B., Marcinkiewicz, M.M. *et al.* (2017) Armc5 deletion causes developmental defects and compromises T-cell immune responses. *Nat. Commun.*, **8**, 13834.
12. Hsiao, H.P., Kirschner, L.S., Bourdeau, I., Keil, M.F., Boikos, S.A., Verma, S., Robinson-White, A.J., Nesterova, M., Lacroix, A. and Stratakis, C.A. (2009) Clinical and genetic heterogeneity, overlap with other tumor syndromes, and atypical glucocorticoid hormone secretion in adrenocorticotropin-independent macronodular adrenal hyperplasia compared with other adrenocortical tumors. *J. Clin. Endocrinol. Netab.*, **94**, 2930–2937.
13. Lacroix, A. (2009) ACTH-independent macronodular adrenal hyperplasia. *Best Pract. Res. Clin. Endocrinol. Metab.*, **23**, 245–259.
14. Huelsken, J., Vogel, R., Brinkmann, V., Erdmann, B., Birchmeier, C. and Birchmeier, W. (2000) Requirement for beta-catenin in anterior-posterior axis formation in mice. *J. Cell Biol.*, **148**, 567–578.
15. Haegel, H., Larue, L., Ohsugi, M., Fedorov, L., Herrenknecht, K. and Kemler, R. (1995) Lack of beta-catenin affects mouse development at gastrulation. *Development*, **121**, 3529–3537.
16. Lickert, H., Cox, B., Wehrle, C., Taketo, M.M., Kemler, R. and Rossant, J. (2005) Dissecting Wnt/beta-catenin signaling during gastrulation using RNA interference in mouse embryos. *Development*, **132**, 2599–2609.
17. El Wakil, A. and Lalli, E. (2011) The Wnt/beta-catenin pathway in adrenocortical development and cancer. *Mol. Cell. Endocrinol.*, **332**, 32–37.
18. Berthon, A., Martinez, A., Bertherat, J. and Val, P. (2012) Catenin signalling in adrenal physiology and tumour development. *Mol. Cell. Endocrinol.*, **351**, 87–95.
19. Berthon, A., Sahut-Barnola, I., Lambert-Langlais, S., de Joussineau, C., Damon-Soubeyrand, C., Louiset, E., Taketo, M.M., Tissier, F., Bertherat, J., Lefrancois-Martinez, A.M. *et al.* (2010) Constitutive beta-catenin activation induces adrenal hyperplasia and promotes adrenal cancer development. *Hum. Mol. Genet.*, **19**, 1561–1576.
20. Tissier, F., Cavard, C., Groussin, L., Perlemoine, K., Fumey, G., Hagnere, A.M., Rene-Corail, F., Jullian, E., Gicquel, C., Bertagna, X. *et al.* (2005) Mutations of beta-catenin in adrenocortical tumors: activation of the Wnt signaling pathway is a frequent event in both benign and malignant adrenocortical tumors. *Cancer Res.*, **65**, 7622–7627.
21. Bourdeau, I., Antonini, S.R., Lacroix, A., Kirschner, L.S., Matyakhina, L., Lorang, D., Libutti, S.K. and Stratakis, C.A. (2004) Gene array analysis of macronodular adrenal hyperplasia confirms clinical heterogeneity and identifies several candidate genes as molecular mediators. *Oncogene*, **23**, 1575–1585.
22. Bimpaki, E.I., Iliopoulos, D., Moraitis, A. and Stratakis, C.A. (2010) MicroRNA signature in massive macronodular adrenocortical disease and implications for adrenocortical tumourigenesis. *Clin. Endocrinol. (Oxf.)*, **72**, 744–751.
23. Tadjine, M., Lampron, A., Ouadi, L. and Bourdeau, I. (2008) Frequent mutations of beta-catenin gene in sporadic secreting adrenocortical adenomas. *Clin. Endocrinol. (Oxf.)*, **68**, 264–270.
24. Alencar, G.A., Lerario, A.M., Nishi, M.Y., Mariani, B.M., Almeida, M.Q., Tremblay, J., Hamet, P., Bourdeau, I., Zerbini, M.C., Pereira, M.A. *et al.* (2014) ARMC5 mutations are a frequent cause of primary macronodular adrenal hyperplasia. *J. Clin. Endocrinol. Metab.*, **99**, E1501–E1509.
25. Elbelt, U., Trovato, A., Kloth, M., Gentz, E., Finke, R., Spranger, J., Galas, D., Weber, S., Wolf, C., Konig, K. *et al.* (2015) Molecular and clinical evidence for an ARMC5 tumor syndrome: concurrent inactivating germline and somatic mutations are associated with both primary macronodular adrenal hyperplasia and meningioma. *J. Clin. Endocrinol. Metab.*, **100**, E119–E128.
26. Berthon, A., Faucz, F., Bertherat, J. and Stratakis, C.A. (2017) Analysis of ARMC5 expression in human tissues. *Mol. Cell. Endocrinol.*, **441**, 140–145.
27. Griffin, K.J., Kirschner, L.S., Matyakhina, L., Stergiopoulos, S.G., Robinson, W.A., Lenherr, S.M., Weinberg, F.D., Claflin, E.S., Batista, D., Bourdeau, I. *et al.* (2004) A transgenic mouse bearing an antisense construct of regulatory subunit type 1A of protein kinase A develops endocrine and other tumours: comparison with Carney complex and other PRKAR1A induced lesions. *J. Med. Genet.*, **41**, 923–931.
28. Faucz, F.R., Zilbermint, M., Lodish, M.B., Szarek, E., Trivellin, G., Sinaii, N., Berthon, A., Libe, R., Assie, G., Espiard, S. *et al.* (2014) Macronodular adrenal hyperplasia due to mutations in an Armadillo repeat containing 5 (ARMC5) gene: a clinical and genetic investigation. *J. Clin. Endocrinol. Metab.*, **99**, E1113–E1119.